THE ASTROPHYSICAL JOURNAL, 410:668–672, 1993 June 20

SPECTRAL IMAGING OF THE 3.3 AND 11.3 MICRON EMISSION BANDS IN NGC 1333: DISCOVERY OF SPATIALLY SEPARATE BAND EMISSIONS

JESSE BREGMAN,[1] DAVID RANK,[2] SCOTT A. SANDFORD,[1] AND PASQUALE TEMI[2]
Received 1992 August 14; accepted 1992 December 22

ABSTRACT

Spectral images and aperture spectra were obtained of the nebula around the star SVS 3 in the star formation region NGC 1333. The spectra contain strong infrared emission bands originating from carbonaceous material. The spectra show the presence of the characteristic 3.3 and 11.3 μm emission features thought to be associated with C—H stretching and C—H out-of-plane bending modes, respectively, of polycyclic aromatic hydrocarbons (PAHs). The distribution of the 3.3 μm emission is suggestive of limb brightening from the edge of an emitting shell. The 3.3 and 11.3 μm emission features come from spatially distinct regions, with the 3.3 μm emission occurring outside the region of strongest 11.3 μm emission. Thus, the relative band strengths cannot be used to determine the excitation temperature and average size of the molecules. The relative distributions of the 3.3 and 11.3 μm emission features can be understood if the bands arise from PAH molecules of different sizes. Spectra in the 3 μm region of 4 positions around SVS 3, which sample regions of similar excitation, show 3.3 and 3.4 μm emission bands with the same relative intensities. The data mildly favor the identification of the 3.4 μm band with an excited mode of the C—H stretch (i.e., a hot band) or an overtone/combination rather than with the presence of molecular side groups on the PAHs, since the spectra are identical yet sample physically separate regions.

Subject headings: infrared: interstellar: lines — ISM: individual (NGC 1333) — ISM: molecules

1. INTRODUCTION

The infrared spectra of many planetary nebulae, H II regions, galactic nuclei, reflection nebulae, and WC stars are dominated by a set of narrow emission features and broad plateaus which for many years were called the "unidentified infrared bands." These bands have been attributed to several carbon-rich species, including polycyclic aromatic hydrocarbon (PAH) molecules and PAH clusters (Leger & Puget 1984; Allamandola, Tielens, & Barker 1985), hydrogenated amorphous carbon (HAC) particles (Duley & Williams 1981), and quenched carbonaceous composite (QCC) particles (Sakata et al. 1984). All of these suggested materials contain only carbon and hydrogen atoms, and contain or are dominated by aromatic (sp^2) carbon skeletons (Robertson & O'Reilly 1987). If the narrow bands are from PAH molecules, then PAHs contain 1%–10% of the interstellar carbon, making them the most abundant molecular species in the interstellar medium after H_2 and CO.

Bregman et al. (1989) showed that the narrow emission features and underlying broad plateaus had different spatial distributions in the Orion Bar region. On the other hand, the series of narrow bands all had similar spatial distributions. While the narrow bands peaked just outside the ionized region, the broad bands also existed within the ionized region. This behavior suggested that the narrow bands arose from PAH molecules that had shorter lifetimes in the harsh UV field near the Orion Bar than the larger PAH clusters that produced the broader features. Laboratory spectra of PAHs indicated that if the narrow bands were from PAHs, then there should be additional weak bands at 5.2 μm and between 11.3 and 13 μm. These bands were subsequently observed (Allamandola et al. 1989a; Roche, Aitken, & Smith 1989; Witteborn et al. 1989). Thus, there was strong evidence that at least the narrow emission bands were due to PAH molecules. In PAH molecules, the 3.3 μm band is due to a C—H stretch, the 8.6 and 11.3 μm bands are due to C—H bends (in and out of plane, respectively), and the 6.2 and 7.7 μm bands are C—C modes. Allamandola et al. (1985) had also suggested that the bands observed just longward of the 3.3 μm band, the strongest occurring at 3.4 μm were due to excited states of PAH molecules. Following up on this suggestion, Bregman (1989) compared existing data for band ratios for the 3.3, 3.4, and 11.3 μm bands with the ratios expected if all of these bands were due to C—H modes in PAHs. This comparison showed that the data did not fit the theory if the same size PAHs were producing all the bands. One of the difficulties in compiling the observational data and calculating ratios was that the published observations were taken using different sized apertures, and many, if not all, of the sources were extended. For example, Bregman et al. (1992) showed that the apparent point source, IRAS 21282+5050, was extended on a scale of at least 20″. However, a set of data we obtained for a number of sources through the same sized apertures at 3 and 11 μm did not show substantially different behavior than the original sample. The data could be reconciled with PAH emission if the 11.3 μm band was dominated by emission from large PAHs and the 3.3 and 3.4 μm bands were dominated by emission from small PAHs. Theoretical calculations by Schutte, Tielens, & Allamandola (1993) show that this could well be the case.

If, as is expected, the 3.3 μm band arises primarily from small PAHs and the 11.3 μm band from large PAHs, the spatial distributions of these bands can be used to probe the conditions under which different size molecules can survive. To address this question, we have obtained images centered on the B6 star SVS 3 (Harvey, Wilking, & Joy 1984; Strom, Vrba, &

[1] Space Sciences Division, MS 245-6, NASA Ames Research Center, Moffett Field, CA 94035-1000.
[2] UCO and Lick Observatory, University of California at Santa Cruz, Santa Cruz, CA 94035.

Strom 1976) in the star formation region NGC 1333 in both the 3.3 and 11.3 μm emission bands. In § 2 we will discuss the instruments and observations and then discuss the implications of the observations in § 3.

2. OBSERVATIONS AND INSTRUMENT DESCRIPTION

The observations were made with the NASA/University of Arizona 1.5 m telescope on Mount Lemmon in 1991 November. Two infrared cameras were used, one with a 128 × 128 InSb array and the other with a 128 × 128 Si:Ga array. Both arrays were manufactured by Amber Engineering. The cameras have been built with similar liquid helium Dewars, so that either an InSb or a Si:Ga array can be used with common controller and data acquisition electronics. The Si:Ga array requires liquid helium operation, while the InSb detector was operated at pumped liquid nitrogen temperatures. Antireflection coated lens, filter, and widow assemblies are optimized for the bandpass of the two different arrays. Each camera has a filter wheel, a 38 mm f/1.5 ZnSe reimaging lens (operating at a focal reduction of 2), with field and Lyot stop baffles. The InSb camera has 6 fixed filters and the Si:Ga camera has 4 fixed filters and a 1.8% spectral resolution 8–14 μm circular variable filter (CVF). For the 11.3 μm image, NGC 1333 was chopped 90″ north-south at a frequency of 1 Hz. Frames were co-added for 60 s; then the telescope was nodded to allow cancellation of telescope background and offset. For the 3.3 μm image, the data were obtained in a staring mode through a 3.6% wide bandpass filter. The object was observed for 20 s; then the telescope was moved 90″ and the sky was measured. The sequence continued with the sky being sampled and then the object. An optical CCD guide camera and a gold-coated dichroic beamsplitter were used, allowing for accurate guiding with a computer-controlled autoguider. The autoguider reduces image motion to a fraction of an arcsecond, and ensures that the image is returned to the same place on the infrared array during nodding of the telescope.

Figure 1 (Plate 8) is a combination of the 3.3 and 11.3 μm images of NGC 1333 guided on SVS 3 (Strom et al. 1976). The 3.3 μm data are shown in contour intervals of 5.5 mJy arcsec^{-2}, with the lowest contour ar 5.5 mJy arcsec^{-2}. The 11.3 μm image is displayed in color with blue indicating low brightness and red high brightness, with a peak intensity of 140 mJy arcsec^{-2}. The 3.3 μm image is the sum of 10 20 s on-source images after subtracting 10 interlaced sky images. The 11.3 μm image is the sum of 32 chopped and nodded images, each the difference of 60 0.37 s source and 60 0.37 s sky frames. Unchopped sky background frames were used to flat-field the images. The images were then smoothed with a Gaussian function with a full width at half-maximum of 2 pixels (2″ for the 11.3 μm image and 1″.5 for the 3.3 μm image). The two images were registered using SVS 3 and positioning information from the autoguider. Rotation of each of the two cameras was measured by trailing a star north-south across the array while taking a long integration. The measured rotation relative to the north-south direction was 0° for the InSb camera and 3°.5 west of north (clockwise) for the Si:Ga camera. The 11.3 μm image was rotated 3°.5 counterclockwise before registration with the 3.3 μm image. A K-band image was also obtained to check that the knots of 3.3 μm emission were not due to foreground or background stars. Only SVS 3 was visible on the K-band image.

In addition to the spectral images, aperture spectra were obtained from the NASA 1.5 m telescope in 1989 October at several locations in the nebula, both from 3 to 4 μm and from 10.5 to 11.5 μm, using two grating spectrometers with InSb and Si:Bi linear arrays, respectively. Instrument descriptions can be found in Witteborn & Bregman (1984) and Wooden (1989). Both spectrometers used 12″ apertures and chopper throws of 70″ in declination. Standard nodding techniques were used to remove telescope offset. The 3.3 μm band was measured at the five aperture positions shown in Figure 2, and the resultant spectra are shown in Figure 3. The 11.3 μm band was measured at two locations, one centered on SVS 3 and one centered 10″ south of SVS 3. These spectra are shown in Figure 4. While the positions where the spectra were taken are shown in Figure 2 as sharp circles, in reality the spectrometer aperature does not have a sharp cutoff. Also, guiding errors move the aperature around on the source. These two effects combine to produce an effective aperture somewhat larger than indicated. The lack of continuum emission in the spectra from all but the central spectrum of Figure 3 shows that (except for the stellar contribution from SVS 3) the emission at 3.3 μm comes entirely from a narrow infrared emission band. The spectra shown in Figure 4 shows that the 11.3 μm emission also comes almost entirely from a narrow infrared emission band. Thus, the spectral images give a good indication of the distribution of the PAH emission.

3. DISCUSSION

Since the 3.3 and 11.3 μm bands are both thought to be due to C—H modes (C—H stretch versus C—H bend) of the same molecular bonds in the PAHs, it has been generally assumed that their relative strengths, when observed through similar size apertures, can be compared and used to check theoretical predictions. However, these data call this assumption into question, since, at least in NGC 1333, emission from the C—H mode bands is not spatially coincident. Figure 1 shows that the 3.3 μm band emission, at positions other than near the central star, occurs outside the region of maximum 11.3 μm emission, presumably where the intensity of the UV radiation field is rapidly diminishing. The spatial distribution of the 3.3 μm emission is suggestive of limb brightening from a shell, since

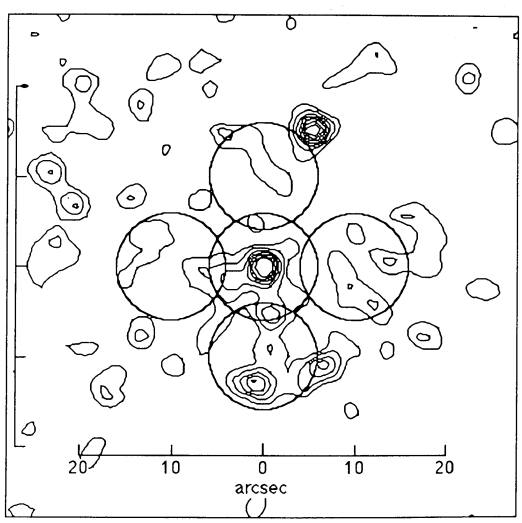

FIG. 2.—Aperture FWHM and positions where 3.0–3.7 μm spectra were taken are shown superposed on the 3.3 μm emission intensity contours. The tick marks along the east and south edges are spaced every 10″.

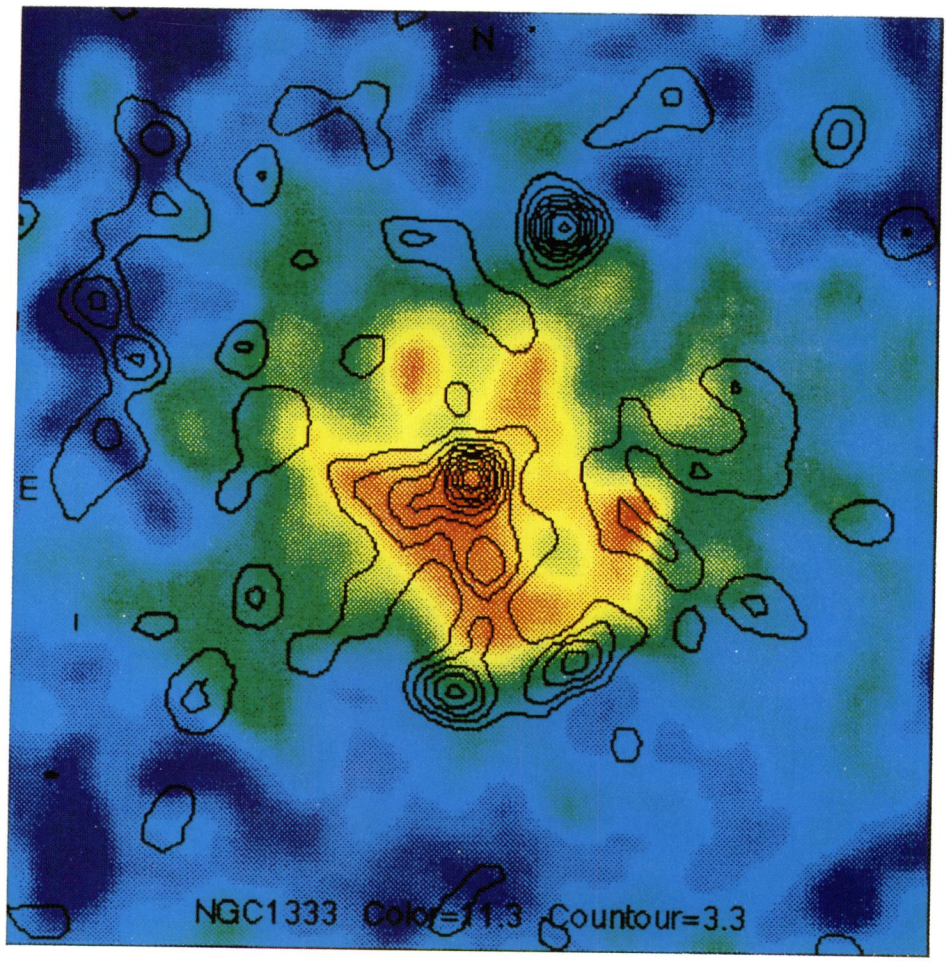

FIG. 1.—The 11.3 μm emission around the star SVS 3 in NGC 1333 (contour peak near the center) is shown in color, with red indicating the maximum brightness (140 mJy arcsec^{-2}) and blue the minimum brightness. The contours show the distribution of 3.3 μm emission. The lowest 3.3 μm contour is 5.5 mJy arcsec^{-2}, and the contours are spaced at equal intervals of 5.5 mJy arcsec^{-2}. North is up, and east is to the left. The full extent of the map is a 64 × 64 section of the Si:Ga 128 × 128 detector array and has a scale of 0.″96 pixel^{-1}. The distance along each side is 61.″4.

BREGMAN, RANK, SANDFORD & TEMI (see 410, 669)

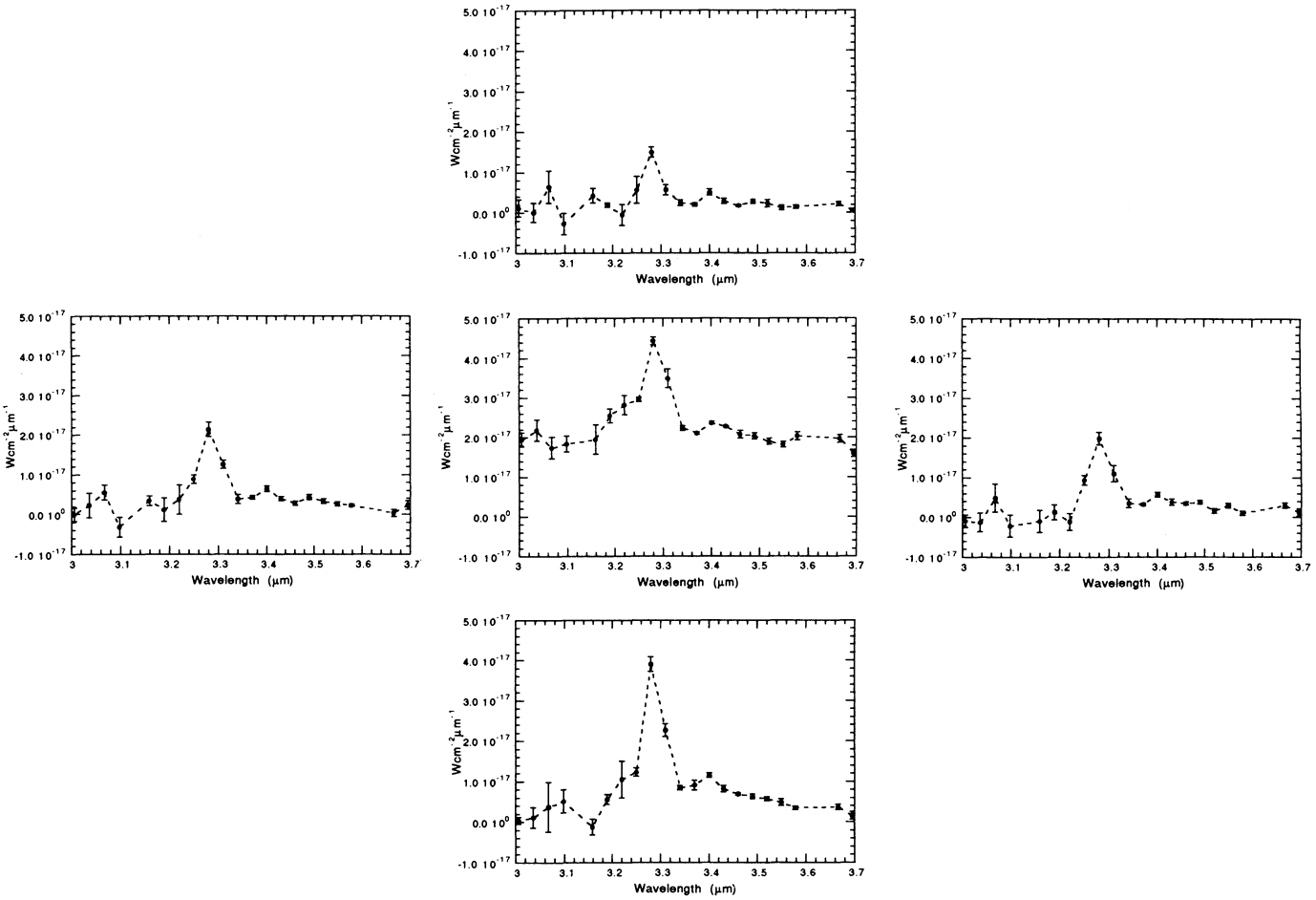

FIG. 3.—The 3.0–3.7 μm spectra for each of the five aperture positions indicated on Fig. 2

the strongest peaks fall very close to a circle centered on SVS 3. The 3.3 μm emission near SVS 3 would presumably be in front of or behind the exciting star.

Various authors (e.g., Allamandola et al. 1985; de Muizon et al. 1986; Cohen et al. 1989; Leger, d'Hendecourt, & Defourneau 1989) have used the ratio of the 3.3 and 11.3 μm bands measured with single-aperture spectrometers to estimate the size of the PAHs producing the observed emission in a variety of objects. All of these estimates assume that both features originate from the same C—H bonds on the same molecules. However, the spatial distribution of the two bands shown in Figure 1 clearly demonstrates that the bands do not originate from the same molecules or even from the same spatial location. Thus, the previous molecular size constraints derived

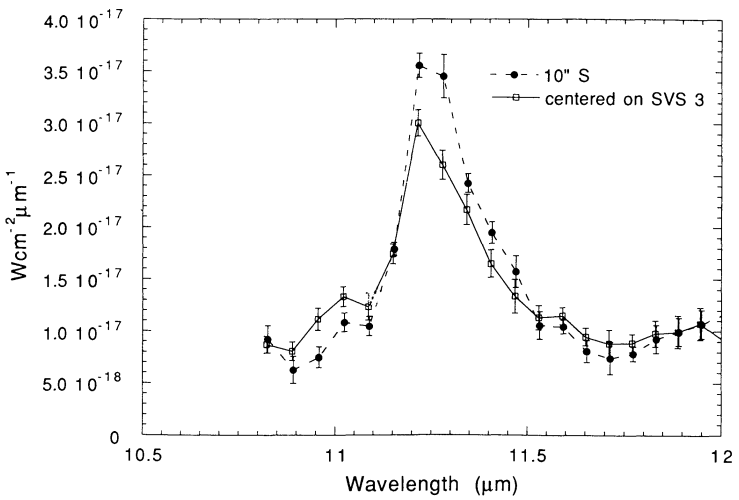

FIG. 4.—The 11.3 μm emission band is shown for two positions in NGC 1333

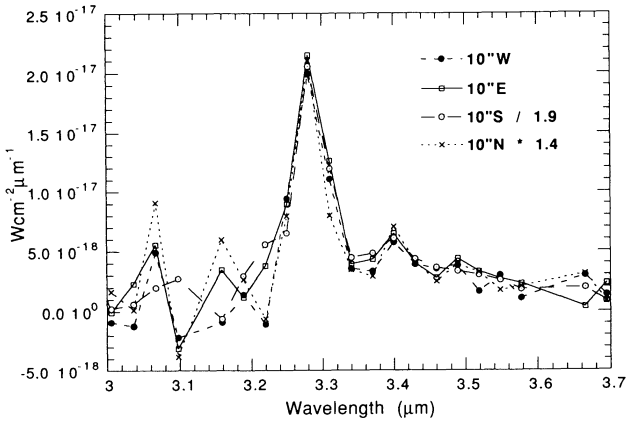

FIG. 5a

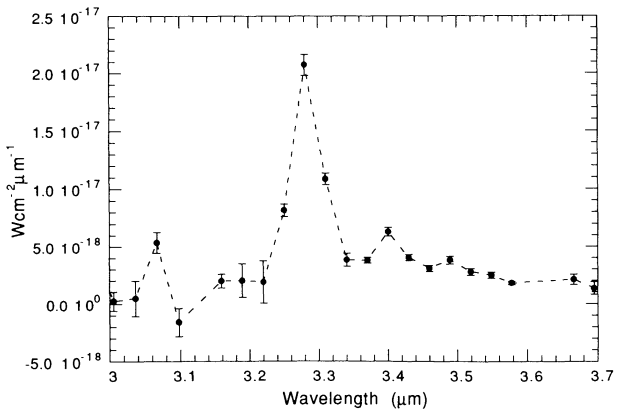

FIG. 5b

FIG. 5.—(*a*) Comparison of the four off-star spectra around SVS 3. All the spectra have been scaled to a similar intensity at 3.28 μm. The 10″ south position has been divided by 1.9, and the 10″ north position has been multiplied by 1.4. The east and west positions were not scaled. (*b*) Average of the four scaled spectra shown in (*a*).

from 3.3 μm/11.3 μm band ratios are called into question, and may very well be entirely wrong.

The 3 μm spectral profiles at the four positions around SVS 3 are remarkably similar. Figure 5 shows a superposition of normalized spectra from the four positions and their average. The 3.4 and 3.5 μm bands that are prominent in other objects (cf. de Muizon et al. 1986) are also present in these data. These bands have been attributed to higher excitation C—H stretch modes (hot bands) and ovetone/combination modes (Barker, Allamandola, & Tielens 1987; Sandford 1991), to linear side groups attached to PAH rings (de Muizon et al. 1986), and to linear side groups attached to large amorphous carbon particles (Duley & Williams 1981).

Recently, Geballe et al. (1992) have observed 3.3/3.4 μm band ratios near unity in some post–asymptotic giant branch (post-AGB) stars, supporting the side-group explanation. However, they point out that it is not clear whether the 3.4 μm band they observe in the post-AGB stars, where there is little UV radiation, has the same origin as in regions with strong UV radiation fields. Certainly, in strong UV radiation fields like that of NGC 7027, the side-group model fails to explain the 3–4 μm spectrum (Sandford 1991).

In our data, the excitation is presumably the same at all four positions around SVS 3, since the 3.3 μm emission appears to occur at the same distance from the exciting star at all the locations. Since the four positions also sample different knots of material, it would be possible for the chemistry at each location to be different and the mixture of side groups need not be the same at each location. Thus, the similarity of the spectra at all of the locations mildly favors the explanation that this emission is due to hot bands and overtone/combinations, although side groups cannot be ruled out.

It is possible to understand our spectral image observations if PAHs are the source of the emission bands and if PAHs are dehydrogenated by the UV radiation field. Because of the molecular energetics of UV-excited PAHs, the 3.3 μm band is expected to be dominated by the smallest PAHs present, while the 11.3 μm band should originate primarily from larger PAHs (Schutte et al. 1993). The dehydrogenation rate for PAHs is a strong function of the number of carbon atoms in the molecule, with the dehydrogenation rate being larger for small PAHs than for large PAHs (Allamandola, Tielens, & Barker 1989b). The rehydrogenation rate is a slowly increasing function of the number of carbon atoms in the molecule, since it depends on the gas density and collision cross section of the molecules. Thus, small PAHs remain dehydrogenated close to the exciting star much more easily than large PAHs (cf. Geballe et al. 1989). Only when the intensity of the UV field falls low enough so that the dehydrogenation rate drops below the rehydrogenation rate for small PAHs will the 3.3 μm band become strong. Following Geballe et al. (1989), we can estimate the dehydrogenation and rehydrogenation rates for PAHs in NGC 1333. From Kurucz, Peytremann, & Avrett (1974), we find that the UV photon flux from a 13,000 K star between 912 and 1300 Å is 0.082 of the total luminosity of the star. The distance to NGC 1333 is 500 pc, and SVS 3 has a luminosity of 360 $L_\odot$ (Harvey et al. 1984). Thus, at the edge of the 11.3 μm region where the 3.3 μm band has several peaks (an angular distance of 14″), the UV photon flux is $\approx 3.6 \times 10^{10}$ cm^{-2} s^{-1}. Multiplying this by the UV absorption cross section for 20 C atom PAHs of 5×10^{-16} cm^2 yields an H loss rate of 1.8×10^{-5} s^{-1}. The H loss rate for larger PAHs is much less. The rehydrogenation rate is given by Tielens et al. (1987) as $R = 10^{-9} n$ s^{-1} where n is the gas density. The density in the nebula around SVS 3 has not been measured, but for similar regions is typically $\approx 10^4$ cm^{-3}. Using these values, the rehydrogenation rate is $\approx 10^{-5}$ s^{-1}, or comparable to the dehydrogenation rate 14″ from SVS 3, where the 3.3 μm band emission peaks. Closer to SVS 3, the dehydrogenation rate will be greater than the rehydrogenation rate if the nebula has a density that decreases more slowly with distance from SVS 3 than $1/r^2$. Thus, our spectral images of NGC 1333 are consistent with the explanation that small PAHs dominate the 3.3 μm band emission, large PAHs dominate the 11.3 μm band emission, and the different spatial distribution of these two bands is due to dehydrogenation of the smallest PAHs by UV radiation.

4. CONCLUSIONS

Spectral images in the 3.3 and 11.3 μm infrared emission bands around the star SVS 3 in NGC 1333 show that the two bands originate from spatially different locations. Thus, the ratio of these bands cannot be used to estimate the sizes of the molecules emitting the bands. The data are consistent with the emission bands arising from a mixture of different size PAH molecules in which the smallest PAHs have been dehydrogenated close to SVS 3. Aperture spectra from 3.0 to 3.7 μm at

four positions around SVS 3, which sample regions of similar excitation, show similar ratios between the 3.3 and 3.4 μm emission bands. The similarity of the spectra at these four physically separate regions mildly favors the explanation that hot bands and overtone/combination bands account for the 3.4 μm band rather than molecular side groups on the PAHs.

We wish to thank Doug Hudgins and Laura Kay for their help with the camera observations, and Amara Graps and Fred Witteborn for their assistance in obtaining the spectral data. We are also indebted to the Mount Lemmon and Mount Hamilton staffs for helping to prepare the telescopes for operation.

REFERENCES

Allamandola, L. J., Bregman, J. D., Sandford, S. A., Tielens, A. G. G. M., Witteborn, F. C., Wooden, D. H., & Rank, D. 1989a, ApJ, 345, L59
Allamandola, L. J., Tielens, A. G. G. M., & Barker, J. R. 1985, ApJ, 290, L25
———. 1989b, ApJS, 71, 733
Barker, J. R., Allamandola, L. J., & Tielens, A. G. G. M. 1987, ApJ, 315, L61
Bregman, J. D. 1989, in IAU Symp. 135, Interstellar Dust, ed. L. J. Allamandola & A. G. G. M. Tielens (Dordrecht: Kluwer), 109
Bregman, J. D., Allamandola, L. J., Tielens, A. G. G. M., Geballe, T. R., & Witteborn, F. C. 1989, ApJ, 344, 791
Bregman, J. D., Booth, J., Gilmore, D. K., Kay, L., & Rank, D. 1992, ApJ, 396, 120
Cohen, M., Tielens, A. G. G. M., Bregman, J., Witteborn, F. C., Rank, D. M., Allamandola, L. J., Wooden, D. H., & de Muizon, M. 1989, ApJ, 341, 246
de Muizon, M. Geballe, T. R., d'Hendecourt, L. B., & Bass, F. 1986, ApJ, 306, L105
Duly, W. W., & Williams, D. A. 1981, MNRAS, 196, 269
Geballe, T. R., Tielens, A. G. G. M., Allamandola, L. J., Moorhouse, A., & Brand, P. W. J. L. 1989, ApJ, 341, 278
Geballe, T. R., Tielens, A. G. G. M., Kwok, S., & Hrivnak, B. 1992, ApJ, 387, L89
Harvey, P. M., Wilking, B. A., & Joy, M. 1984, ApJ, 278, 156
Kurucz, R. L., Peytremann, E., & Avrett, E. H. 1974, Blanketed Model Atmospheres for Early Type Stars (Washington DC: SAO)
Leger, A., & Puget, J. L. 1984, A&A, 137, L5
Leger, A., d'Hendecourt, L. B., & Defourneau, D. 1989, A&A, 216, 148
Robertson, J., & O'Reilly, E. P. 1987, Phys. Rev. B, 35, 2946
Roche, P. F., Aitken, D. K., & Smith, C. H. 1989, MNRAS, 236, 485
Sakata, A., Wada, S., Tanabe, T., & Onaka, T. 1984, ApJ, 287, L51
Sandford, S. A. 1991, ApJ, 376, 599
Schutte, W. A., Tielens, A. G. G. M., & Allamandola, L. J. 1993, ApJ, in press
Strom, S. E., Vrba, F. J., & Strom, K. M. 1976, AJ, 81, 314
Tielens, A. G. G. M., Allamandola, L. J., Barker, J. R., & Cohen, M. 1987, in Polycyclic Aromatic Hydrocarbons and Astrophysics, ed. A. Leger, L. d'Hendecourt, & N. Boccara (Dordrecht: Reidel), 273
Witteborn, F. C., & Bregman, J. D. 1984, Proc. SPIE, 509, 123
Witteborn, F. C., Sandford, S. A., Begman, J. D., Allamandola, L. J., Cohen, M., Wooden, D. H., & Graps, A. L. 1989, ApJ, 341, 270
Wooden, D. H. 1989, Ph.D. thesis, Univ. California at Santa Cruz